







Evaluation of Harmonic Currents and Network Impedance using Norton Model in an Unidentified Network Configuration

Mohammad I. Alsharari¹ , Mohammad Z. Ahmed¹ , Wael F. Abu Shehab^{1*} ,
Shehab A. Ali² 

¹Department of Electrical Engineering, College of Engineering, Al-Hussein Bin Talal University, Ma'an, Jordan
E-mail: waelabushehab@ahu.edu.jo

²College of Saber, University of Lahej, Yemen

Received: June 08, 2023

Revised: August 03, 2023

Accepted: August 12, 2023

Abstract— This paper presents a study that focuses on the evaluation of the analysis of harmonic currents emitted by loads and the harmonic impedance of a real electrical network using the Norton model. The primary advantage of employing this model lies in its ability to address scenarios where the complete network configuration, particularly from the distribution side, is not known. By calculating currents and voltages at the supply-side for two different operating conditions, the harmonic current content and the network impedance can be evaluated. To induce variations in operating conditions, a switching shunt capacitor is utilized. The results show that the fifth and the seventh harmonics clearly appear with values of 189.382 A and 135.073 A, respectively, while the other harmonics have values close to zero. The harmonic impedance also shows the presence of the fifth and the seventh harmonics with values of 1865.681 Ω and 4289.3 Ω , respectively. The main contribution of this paper focuses on converting the real electrical network into numerical data that can be accepted by the software. The components of the network model have to be carefully selected to understand the harmonic analysis and to success the simulation, which is conducted using the EMTP-ATPDraw program. The results of this investigation can be used as a database for electrical transmission and distribution companies in case of making any changes in the network, such as installation of new loads or cables, or in case of making measurements.

Keywords— Harmonic current; Harmonic impedance; Norton model, Switching capacitor.

1. INTRODUCTION

Nonlinear electronic devices are extensively employed within power systems, resulting in the generation of distorted current and voltage waveforms. These distortions can have detrimental effects on the overall system performance, including fuse failures, device and breaker malfunctions, communication interference, and increased equipment temperatures [1, 2].

The introduction of capacitors for power factor correction can modify the frequency characteristics of the power system. This alteration can give rise to resonances that amplify transient disturbances and harmonic voltages [3]. When operating conditions change within a specific supply system, the harmonic currents injected at specific nodes may also vary. Several techniques have been employed for harmonic analysis [4-16]. They vary according to their modeling complexity, employed algorithms, and data requirements. One of these techniques uses probabilistic methods [4-7]. However, these methods are too complex to derive for investigation the effect of changes that may occur in electrical networks. Another technique

uses constant current source model [8], which has simple structure and requires less data. However, it is not suitable for networks, where large voltage distortions are present [9]. To obtain more accurate results, voltage dependent current source models have been investigated. Frequency-domain admittance matrix [10] and Norton models [11-14] are among these models. Researchers in [9] show that Norton model gives much better results than the frequency-domain admittance matrix model. In addition, Norton model does not require detailed knowledge of the electrical system and only the data at two different operating condition measurements are needed [12,17]. The Norton model has been employed in much research dealing with harmonic analysis in different applications such as low-voltage installations [18], wind farm modeling [19, 20], and inverter-based unit analyses [21-23].

Fig. 1 can be used to estimate the Norton Model for the distribution system by performing measurements of harmonic voltage (V_h) and harmonic current (I_h) for at least two different operating conditions of the supply system. Changing operating conditions of the supply system can be obtained for example by switching a shunt capacitor, disconnecting a parallel transformer or some other changes that cause a change in the harmonic impedance of the supply system [12-14].

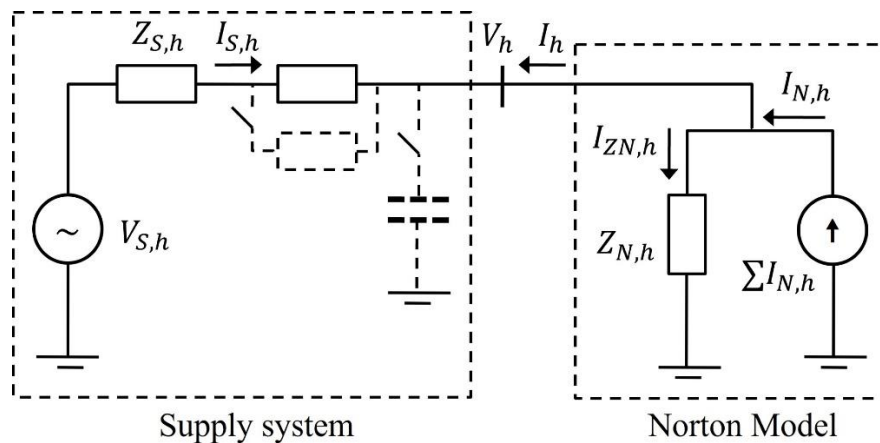


Fig. 1. Norton model of the network.

It has been shown that the harmonic Norton impedance $Z_{N,h}$ and the harmonic Norton current $I_{N,h}$ can be expressed as [12-14]:

$$Z_{N,h} = (V_{h,1} - V_{h,2}) / (I_{h,2} - I_{h,1}) \quad (1)$$

$$I_{N,h} = I_{h,1} + (V_{h,1} / Z_{N,h}) \quad (2)$$

where $V_{h,1}$ and $I_{h,1}$ are harmonic voltage and harmonic current measurements before the operating condition change, and $V_{h,2}$ and $I_{h,2}$ are measurements after the change. It should be mentioned here that Eqs. (1) and (2) are complex and the magnitudes of the harmonic voltage and the harmonic current, in addition to their phase angles, should be precisely determined. Also, it is noted from these equations that no information about the supply system harmonic impedance is needed to calculate $Z_{N,h}$ and $I_{N,h}$.

The use of Norton model was tested on the network connected to Detmarovice power station in Czechia [24] using EMTP-ATPDraw v7.3, which is the graphical preprocessor to the Alternative Transient Program (ATP) version of the Electromagnetic Transients Program

(EMTP) [25]. The main contribution in this paper focuses on converting this real network into numerical data that can be accepted by the software. The components of the network model, which strongly depend on the analyzed problem, have to be carefully selected to understand the harmonic analysis and to success the simulation. The results obtained by EMTP-ATPDraw (currents and voltages) are then drawn by PlotXY software [26], which also offers Fourier transform technique needed for harmonics calculation. Besides PlotXY software, Microsoft Excel is used as well for calculation of harmonic currents and impedance.

The remaining of the paper is organized as follows: In section 2, the studied network is introduced. Network modelling is presented in section 3. Simulation results are discussed in section 4. Finally, section 5 concludes the paper.

2. THE STUDIED NETWORK

The studied network corresponds to a branch of Detmarovice power station (EDE) – block No. 2, located in Czechia, as shown in Fig. 2. This block (EDE2) has synchronous generator with volt-ampere rating of 235 MVA and voltage of 15.75 kV. It supplies a power of 160 MW to 110 kV network via block transformer EDET–15.75/110 kV. 100 MW of this power is consumed in the Kuncice substation (KUN), and 60 MW is fed to 220 kV supergrid of Liskovec (LIS2) via distribution transformer LIST–220/110 kV. Both parts of the power are transferred via the Vratimov substation (VRA). AIFe-110 kV transmission lines are used to connect all the substations. No. 692 single line (two conductors in a bundle $2 \times 670 \text{ mm}^2$, length 20.4 km) is connected between the VRA substation and the EDE station. No. 605-606 double line (240 mm^2 , length 5.168 km) is connected between the VRA substation and the KUN substation, and No. 641-642 double line (450 mm^2 , length 8.107 km) is connected between the VRA substation and the LIS substation.

It will be assumed that the load connected to LIS injects 5th and 7th harmonic currents into the system. Two different operating conditions needed for Norton model estimation will be provided. The switching events must produce significant change in current and voltage, where V_h and I_h are not zeroes. Therefore, the changes will be provided by switching a capacitor (100 MVar) connected to EDET as shown in Fig. 2.

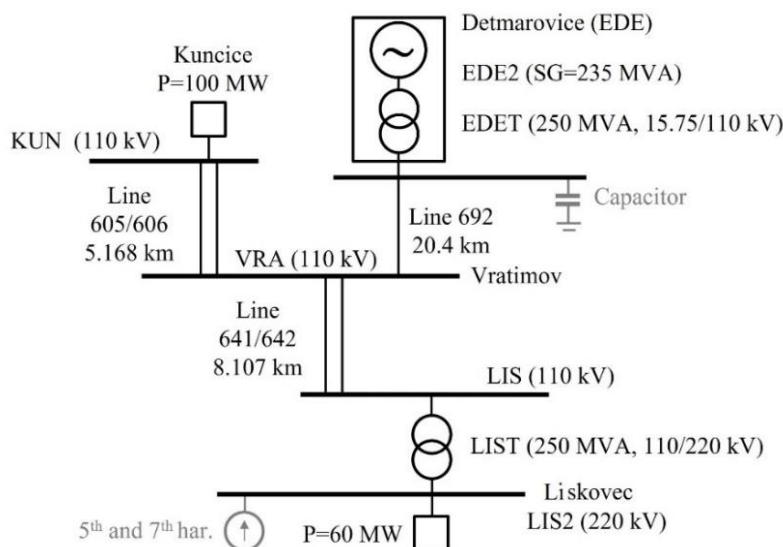


Fig. 2. Scheme of the studied network.

The value of the capacitor is chosen to make significant change in operating conditions. The capacitors, which are used for power factor correction are suitable to be used for such operations.

3. NETWORK MODELLING

The synchronous generator in block No. 2 of Detmarovice power station (EDE2) is modelled in the ATPDraw by SM59 model. The voltage amplitude of the generator is calculated according to Eq. (3), which represents the steady-state voltage at the terminals [24]:

$$V_{amp} = \sqrt{2/3} \times 15.75 = 12.86 \text{ kV} \quad (3)$$

Both transformers in the network: the block transformer EDET and the distribution transformer LIST, which are manufactured by Skoda Plzen in Czechia, are modelled in the ATPDraw by BCTRAN model.

The 110 kV transmission lines are modeled in the ATPDraw by the LCC JMarti model. The single line No. 692 (3-phase) has two conductors in a bundle: length 20.4 km with cross sectional area $2 \times 670 \text{ mm}^2$. The length of the double lines No. 605-606 (3-phase) is 5.168 km with cross sectional area 240 mm^2 . Finally, the length of the double lines No. 641-642 (6-phase) is 8.107 km with cross sectional area 450 mm^2 .

The generator, transformers and transmission lines parameters needed for the mentioned models, in addition to the location of the conductors on the towers for each line, can be found in [24].

Concerning loads, they are modelled in the ATPDraw by the RLC3 model, connected to a grounded star. The values of resistance R , inductance L , and capacitance C of the model are determined by the following equations [12]:

$$R = U^2 / P \quad (4)$$

$$L = U^2 / 2\pi f Q \quad (5)$$

$$C = 0 \quad (6)$$

where U , P , f , and Q are voltage in volts, power in watts, frequency in hertz, and reactive power in volt-amperes reactive, respectively. Q can be calculated by [12]

$$Q = P \tan \alpha \quad (7)$$

where α is phase angle between voltage and current in degrees.

The values of the model are shown in Table 1.

Table 1. Parameters of the loads.

Load	P [MW]	Q [MVar]	$\cos \alpha$	R [Ω]	L [mH]
KUN (110 kV)	100	48.43	0.90	121	796
LIS2 (220 kV)	60	29.06	0.90	806.7	5304

Harmonic source is modelled by HFS_Sour, type 14. It injects 5th and 7th harmonic currents with amplitudes of 100 A and 70 A, respectively.

Finally, the switching capacitor with reactive power of 100 MVA_r is modelled in the ATPDraw by the RLC-3Y model. The value of the phase capacitance is calculated by [12]:

$$C = Q/2\pi fU^2 \quad (8)$$

where a value of 26.3 μF is obtained when Q , f , and U are substituted by 100 MVA_r , 50 Hz , and 110 kV , respectively.

It is important to mention here that end time of simulation T_{max} and time step ΔT must be correctly set in ATPDraw simulation settings to get clear and satisfied results [27]. In the simulation, they were set to 0.2 s and 0.1 μs , respectively. A greater value of T_{max} will be better for FFT, but this is at the expense of x-axis length (longer) and graph unclarity. A smaller value of ΔT means longer calculation time (this needs computer with high processing capability), whereas a greater value of ΔT gives unclear figures.

Using all the models mentioned above, the studied network in Fig. 2 will be modelled as shown in Fig. 3.

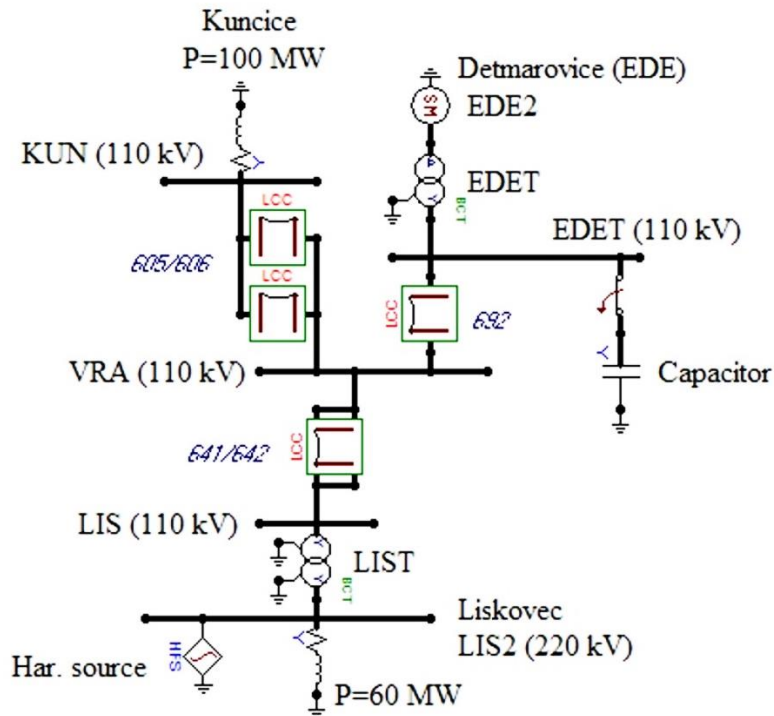


Fig. 3. The EMTP-ATPDraw network model.

4. RESULTS AND DISCUSSION

The harmonic content of the current flowing from EDET-110 kV and the voltage at it will be investigated. Fast Fourier transform (FFT), included in PlotXY, is performed to distinguish the harmonic components of the voltages and currents, with their phase angles, needed for Norton model calculation according to Eqs. (1) and (2). For illustration purposes, the simulation will be done just for phase A. The time window for FFT, the amplitude, and the number of harmonics were set to 0.18-0.2, 70%, and 30, respectively.

The waveform of the current flowing from EDET, before disconnecting the capacitor, is shown in Fig. 4. Its harmonic spectrum obtained by FFT is shown in Fig. 5, which contains the 5th and 7th harmonics. Similarly, Fig. 6 and Fig 7. show the voltage waveform at EDET, before disconnecting the capacitor, and its harmonic spectrum, respectively.

The values (magnitude and phase shift) of the harmonic current and voltage of order h ($h = 1$ to 30), before disconnecting the capacitor, are listed in Table 2 and Table 3, respectively, where THD [%] indicates total harmonic distortion.

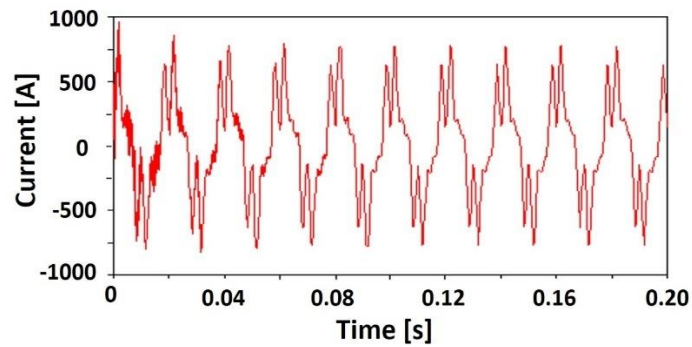


Fig. 4. Waveform of current flowing from EDET before disconnecting the capacitor.

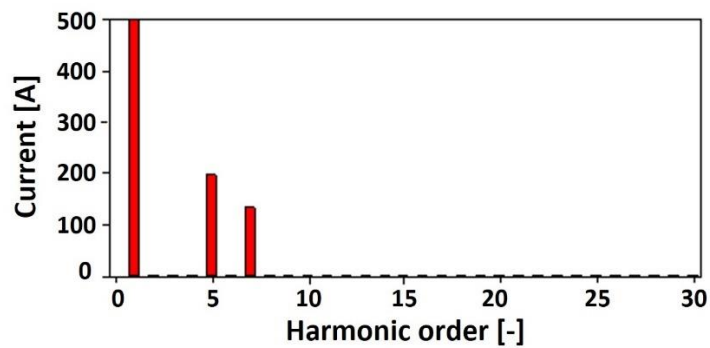


Fig. 5. Harmonic spectrum of the current of Fig. 4.

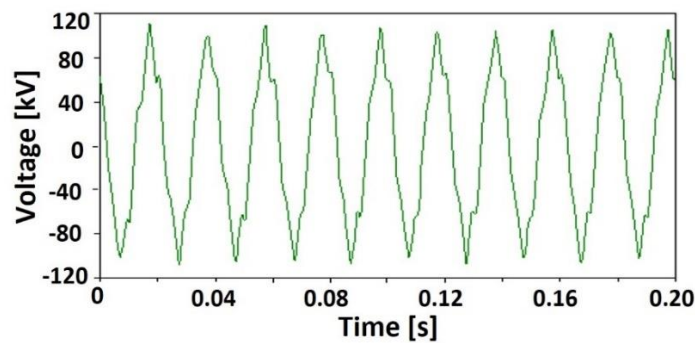


Fig. 6. Voltage waveform at EDET before disconnecting the capacitor.

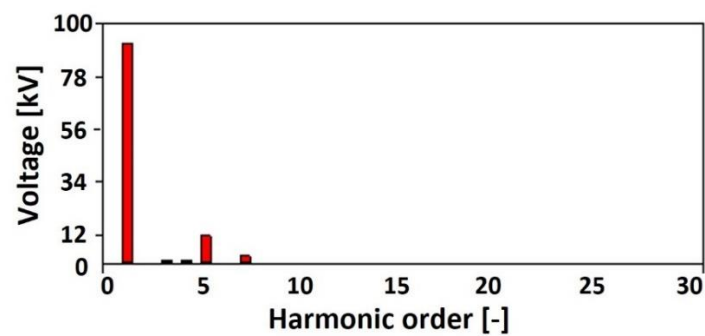


Fig. 7. Harmonic spectrum of the voltage of Fig. 6.

Table 2. Harmonic current flowing from EDET before disconnecting the capacitor.

h	Mag. [A]	Phase [°]	h	Mag. [A]	Phase [°]	h	Mag. [A]	Phase [°]
1	498.650	72.641	11	0.194	-40.897	21	0.070	-13.857
2	0.524	97.764	12	0.162	-36.336	22	0.067	-12.133
3	1.701	132.060	13	0.140	-32.543	23	0.063	-10.444
4	1.423	145.370	14	0.124	-29.292	24	0.060	-8.767
5	195.210	-89.122	15	0.111	-26.443	25	0.057	-7.079
6	0.477	12.808	16	0.101	-23.901	26	0.055	-5.356
7	134.380	-89.456	17	0.093	-21.596	27	0.053	-3.566
8	0.591	-65.933	18	0.086	-19.477	28	0.051	-1.682
9	0.337	-54.282	19	0.080	-17.502	29	0.049	0.339
10	0.244	-46.613	20	0.075	-15.638	30	0.047	2.547

THD = 47.53 %

Table 3. Harmonic voltage at EDET before disconnecting the capacitor.

h	Mag. [V]	Phase [°]	h	Mag. [V]	Phase [°]	h	Mag. [V]	Phase [°]
1	91525.00	136.820	11	57.075	73.830	21	14.850	64.181
2	348.550	-100.620	12	46.792	72.946	22	13.606	63.247
3	1167.800	-125.110	13	39.211	72.003	23	12.528	62.331
4	1426.600	-100.070	14	33.439	71.028	24	11.586	61.434
5	11733	6.267	15	28.930	70.039	25	10.759	60.554
6	340.240	81.935	16	25.332	69.045	26	10.028	59.696
7	3174.900	3.865	17	22.410	68.054	27	9.379	58.857
8	129.520	74.433	18	20.003	67.068	28	8.799	58.039
9	93.556	75.027	19	17.993	66.093	29	8.278	57.242
10	71.630	74.593	20	16.296	65.130	30	7.809	56.470

THD = 13.445 %

To get two different operating conditions, disconnection time of the capacitor has been set to 0.05 s. Fig. 8 shows the waveform of the current flowing from EDET, after disconnecting the capacitor, whereas Fig. 9 shows its harmonic spectrum. Fig. 10 and Fig 11. show the voltage waveform at EDET, after disconnecting the capacitor, and its harmonic spectrum, respectively. The values of the harmonic current and voltage of order h are listed in Table 4 and Table 5, respectively.

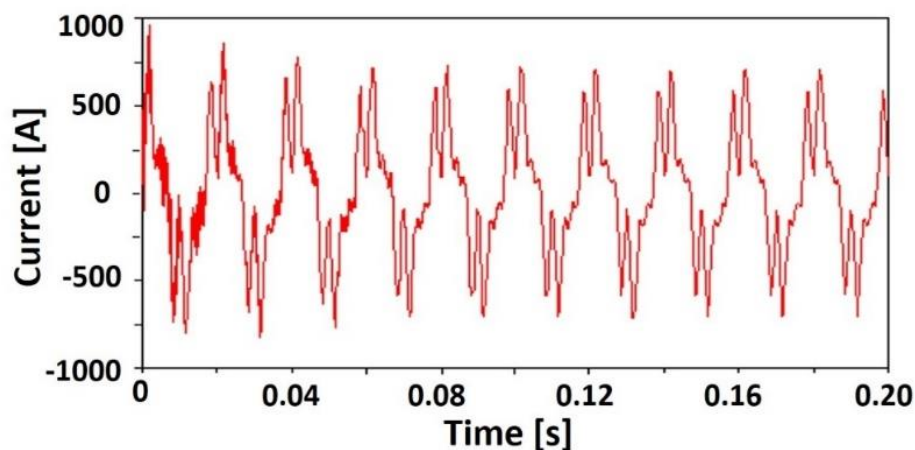


Fig. 8. Waveform of current flowing from EDET after disconnecting the capacitor.

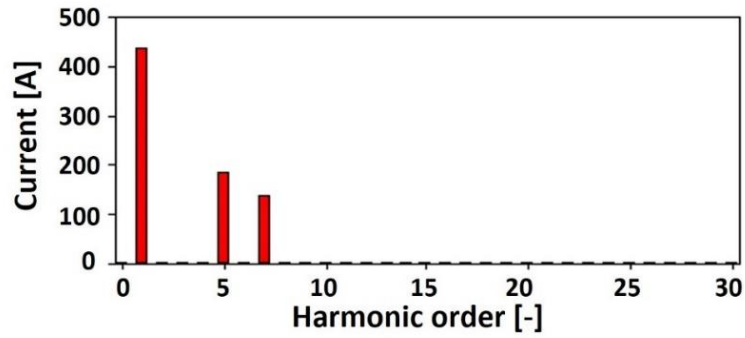


Fig. 9. Harmonic spectrum of the current of Fig. 8.

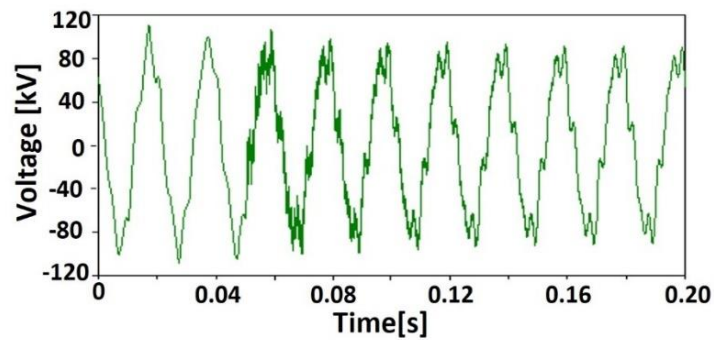


Fig. 10. Voltage waveform at EDET after disconnecting the capacitor.

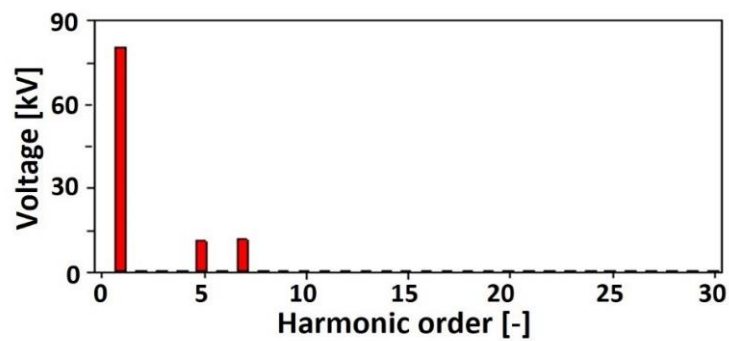


Fig. 11. Harmonic spectrum of the voltage of Fig. 10.

Table 4. Harmonic current flowing from EDET after disconnecting the capacitor.

h	Mag. [A]	Phase [°]	h	Mag. [A]	Phase [°]	h	Mag. [A]	Phase [°]
1	435.63	73.357	11	0.181	-88.965	21	0.116	32.144
2	0.321	80.774	12	0.154	-89.217	22	0.065	29.319
3	0.425	85.489	13	0.138	-89.594	23	0.044	24.515
4	0.684	88.017	14	0.132	-89.993	24	0.033	19.000
5	183.83	-90.311	15	0.135	-90.174	25	0.027	13.452
6	0.071	81.630	16	0.153	-89.649	26	0.023	8.232
7	137.48	-90.025	17	0.220	-86.066	27	0.020	3.449
8	0.598	-89.318	18	1.027	-85.636	28	0.018	6.745
9	0.324	-89.540	19	0.519	165.330	29	0.018	-2.097
10	0.230	-88.880	20	0.416	33.397	30	0.017	-5.538
THD = 52.697 %								

Table 5. Harmonic voltage at EDET after disconnecting the capacitor.

h	Mag. [V]	Phase [°]	h	Mag. [V]	Phase [°]	h	Mag. [V]	Phase [°]
1	80129.000	137.400	11	22.446	-170.430	21	38.733	-57.115
2	20.623	-10.796	12	20.999	-170.230	22	24.376	-58.852
3	19.934	-6.340	13	20.775	-170.710	23	18.441	-61.910
4	37.767	-7.021	14	21.756	-171.720	24	15.321	-65.257
5	10769.000	179.470	15	24.458	-173.020	25	13.445	-68.472
6	9.486	-26.332	16	30.623	-174.210	26	12.219	-71.394
7	11334.000	179.800	17	48.800	-172.510	27	11.348	-73.977
8	54.100	-175.790	18	253.180	-175.110	28	10.641	-73.933
9	29.223	-178.320	19	136.150	73.864	29	10.502	-77.832
10	25.704	-171.360	20	122.140	-56.563	30	10.148	-79.665

THD = 19.516 %

Finally, the data needed for Norton model calculation, according to complex number Eqs. (1) and (2), are obtained. The estimated harmonic currents and the harmonic impedance of the network are listed in Table 6 and Table 7, respectively. From Table 6, it is obvious that values of the 5th and 7th harmonic currents are about 189 A and 135 A, respectively, while the other harmonics have values close to zero. Table 7 and Fig. 12 show the harmonic impedance, where the presence of the 5th and 7th harmonics with values of 1865.681 Ω and 4289.3 Ω , respectively, is clearly shown.

Table 6. Estimated harmonic currents.

h	Mag. [A]	Phase [°]	h	Mag. [A]	Phase [°]	h	Mag. [A]	Phase [°]
1	11.154	-150.65	11	0.209	-76.90	21	0.092	-3.48
2	0.331	79.03	12	0.178	-74.10	22	0.074	2.13
3	0.450	85.41	13	0.160	-70.82	23	0.061	5.02
4	0.716	88.04	14	0.149	-66.75	24	0.053	6.41
5	189.382	-89.83	15	0.145	-61.31	25	0.047	7.12
6	0.084	80.59	16	0.146	-53.58	26	0.043	7.61
7	135.073	-89.57	17	0.150	-41.70	27	0.040	8.19
8	0.653	-83.53	18	0.160	-25.27	28	0.037	11.42
9	0.365	-83.24	19	0.171	-20.96	29	0.036	9.77
10	0.262	-79.39	20	0.121	-13.53	30	0.034	10.90

Table 7. Estimated harmonic impedance.

h	Z [Ω]	Phase [°]	h	Z [Ω]	Phase [°]	h	Z [Ω]	Phase [°]
1	180.584	-114.96	11	455.396	-143.82	21	575.237	38.22
2	1480.304	-45.24	12	420.785	-149.63	22	723.978	0.37
3	816.586	-90.39	13	391.795	-156.98	23	744.217	-30.58
4	1190.197	-95.62	14	367.212	-166.44	24	704.579	-52.08
5	1865.681	-106.34	15	346.550	-179.08	25	659.250	-67.11
6	752.265	-101.02	16	329.268	163.19	26	620.847	-78.27
7	4289.300	113.96	17	316.842	136.55	27	586.857	-87.19
8	648.573	-138.58	18	264.454	98.91	28	531.537	-89.45
9	527.388	-134.96	19	197.761	90.09	29	566.735	-99.28
10	498.274	-139.37	20	353.932	75.23	30	546.994	-105.66



Fig. 12. Estimated harmonic impedance of the network.

5. CONCLUSIONS

The content of harmonics flowing from loads in distribution networks was investigated by measuring currents and voltages at the supply system side for two different operating conditions. It was shown that there is no need to seek data concerning the content of distribution loads, since the two easy measurements provide estimation of the Norton model, from which harmonic currents and harmonic impedance of the network are determined. Different operating conditions are obtained by switching a $26.3 \mu F$ capacitor at the supply side, which results in measuring harmonic currents and voltages for two cases: before and after disconnecting the capacitor. The harmonic content of the current injected to the network was obtained, and the harmonic impedance of the network was estimated. Obtaining the values for the components of the real electrical network, in order to construct it in the ATPDraw, was a challenging aspect of this investigation. Since the calculations provided in this paper simulate a real network, accuracy is highly required. Any errors in the calculations would result in a useless and ineffective database. The results of this work can be used as a database for electrical transmission and distribution companies in case of making any changes in the network, such as installation of new loads or cables, or in case of making measurements. To validate the calculation results, a single measurement is sufficient for comparison purposes, from which a rich database can be obtained.

REFERENCES

- [1] J. Silva, V. Sousa, P. Sarmiento, J. Gomez, P. Viego, E. Quispe, "Effects of power electronics devices on the energy quality of an administrative building," *International Journal of Power Electronics and Drive System*, vol. 10, no. 4, pp. 1951-1960, 2019, doi: 10.11591/ijpeds.v10.i4.pp1951-1960.
- [2] G. Singh, "Electric power quality-issues, effects and mitigation," *International Journal of Engineering Research and Technology*, vol. 2, no. 6, pp. 933-944, 2013, doi: 10.17577/IJERTV2IS60396.
- [3] S. Mohamed, M. Alarfaj, M. Shwehdi, A. Bubshait, A. Smadi, "Investigation of harmonics and transient over voltages due to capacitor bank switching on distribution network," *International Journal of Advance Science and Technology*, vol. 29, no. 10s, pp. 7947-7957, 2020, <http://sersc.org/journals/index.php/IJAST/article/view/24240>.
- [4] X. Xiao, R. Zhou, X. Ma, R. Xu, "A novel method for estimating utility harmonic impedance based probabilistic evaluation," *IET Generation, Transmission and Distribution*, vol. 16, no. 7, pp. 1438- 1448, 2022, doi: 10.1049/gtd2.12380.

- [5] S. Heunis, R. Herman, "A probabilistic model for residential consumer loads," *IEEE Transactions on Power Systems*, vol. 17, no. 3, pp. 621-625, 2002, doi: 10.1109/TPWRS.2002.800901.
- [6] Q. Shu, S. Zhao, F. Xu, "Novel estimation method of utility harmonic impedance based on short-term impedance minimum variance criterion," *IET Generation, Transmission and Distribution*, vol. 14, no. 15, pp. 2951-2958, 2020, doi: 10.1049/iet-gtd.2019.1323.
- [7] Z. Tang, H. Li, F. Xu, Q. Shu, Y. Jiang, "A Harmonic impedance estimation method based on the cauchy mixed model," *Mathematical Problems in Engineering*, vol. 2020, pp. 1-13, 2020, doi: 10.1155/2020/1580475.
- [8] W. Xu, "Component modeling issues for power quality assessment," *IEEE Power Engineering Review*, vol. 21, no.11, pp. 12-17, 2001, doi: 10.1109/MPER.2001.961998.
- [9] M. Balci, D. Ozturk, O. Karacasu, M. Hocaoglu, "Experimental verification of harmonic load models," *43rd International Universities Power Engineering Conference*, 2008, doi: 10.1109/UPEC.2008.4651607.
- [10] J. Yong, L. Chen, A. Nassif, W. Xu, "A frequency-domain harmonic model for compact fluorescent lamps," *IEEE Transactions on Power Delivery*, vol. 25, no. 2, pp. 1182-1189, 2010, doi: 10.1109/TPWRD.2009.2032915.
- [11] D. Bilandzija, M. Barukcic, V. Corluca, "Using an evolutionary algorithm for harmonic load modeling by Norton and Thevenin equivalents," *International Journal of Electrical and Computer Engineering Systems*, vol. 5, no. 2, pp. 39-45, 2014.
- [12] S. Ali, "A Norton model of a distribution network for harmonic evaluation," *Energy Science and Technology*, vol. 2, no. 1, pp. 11-17, 2011, doi: 10.3968/j.est.1923847920110201.
- [13] M. Ghorbani, S. Atashpar, A. Mehrafrooz, H. Mokhtari, "Nonlinear loads effect on harmonic distortion and losses of distribution networks," *26th International Power System Conference*, 2011, doi:10.13140/2.1.5047.3288.
- [14] M. Ghorbani, H. Mokhtari, "Impact of harmonics on power quality and losses in power distribution systems," *International Journal of Electrical and Computer Engineering*, vol. 5, no. 1, pp. 166-174, 2015, doi:10.11591/ijece.v5i1.pp166-174.
- [15] E. Almaita, "An adaptive real-time technique for harmonics estimation using adaptive radial basis function neural network," *Jordan Journal of Electrical Engineering*, vol. 8, no. 4, pp. 395-410, 2022, doi: 10.5455/jjee.204-1664801825.
- [16] K. Alawasaa, A. Al-Mbaideen, "Power quality assessment and analysis for low voltage distribution networks," *Jordan Journal of Electrical Engineering*, vol. 4, no. 3, pp. 165-175, 2018.
- [17] M. Ghorbani, M. Rad, H. Mokhtari, M. Honarmand, M. Youhannaie, "Residential loads modeling by Norton equivalent model of household loads," *Asia-Pacific Power and Energy Engineering Conference*, 2011, doi: 10.1109/APPEEC.2011.5748819.
- [18] T. Busatto, V. Ravindran, A. Larsson, S. Ronnberg, M. Bollen, J. Meyer, "Deviations between the commonly-used model and measurements of harmonic distortion in low-voltage installations," *Electric Power Systems Research*, vol. 180, p. 106166, 2020, doi: 10.1016/j.epsr.2019.106166.
- [19] J. Zhao, H. Yang, A. Pan, F. Xu, "An improved complex ICA based method for wind farm harmonic emission levels evaluation," *Electric Power Systems Research*, vol. 179, p. 106105, 2020, doi: 10.1016/j.epsr.2019.106105.
- [20] Y. Zhao, J. Milanovic, "Equivalent modelling of wind farms for probabilistic harmonic propagation studies," *IEEE Transactions on Power Delivery*, vol. 37, no. 1, pp. 603-611, 2022, doi: 10.1109/TPWRD.2021.3065888.
- [21] Z. Deng, G. Todeschini, K. Koo, "Comparison between ideal and frequency-dependent Norton equivalent model of inverter-based resources for harmonic studies," *IEEE PES Innovative Smart Grid Technologies - Asia*, 2021, doi: 10.1109/ISGTAsia49270.2021.9715634.

- [22] S. Muller, J. Meyer, P. Schegner, "Extended coupled Norton model of modern power-electronic devices for large-scale harmonic studies in distribution networks," *IET Power Electronics*, vol. 13, no. 13, pp. 2706-2714, 2020, doi: 10.1049/iet-pel.2019.1444.
- [23] C. Rojas, S. Kouro, R. Inzunza, Y. Mitsugi, A. Alcaide, "Harmonic impedance model of multiple utility-interactive multilevel photovoltaic inverters," *Energies*, vol. 15, no. 24, p. 9462, 2022, doi: 10.3390/en15249462.
- [24] S. Ali, "Study of short-circuit currents around detmarovice power station," *Transactions on Electrical and Electronic Materials*, vol. 15, no. 3, pp. 117-124, 2014, doi: 10.4313/TEEM.2014.15.3.117.
- [25] H. Hoidalén, L. Prikler, F. Penaloza, "ATPDraw version 7.3 for windows- users' manual," *Norwegian University of Science and Technology (NTNU)*, Norway, 2021, https://atp-empt.org/downloads_users.php.
- [26] M. Ceraolo, "MC's PlotXY – A general-purpose plotting and post-processing open-source tool," *SoftwareX*, vol. 9, pp. 282-287, 2019, doi: 10.1016/j.softx.2019.01.017.
- [27] W. Abu Shehab, S. Ali, M. Alsharari, "Lightning protection for power transformers of Aqaba thermal power station," *Archives of Electrical Engineering*, vol. 69, no. 3, pp. 645-660, 2020, doi:10.24425/aee.2020.133923.